A&A 448, 853–860 (2006)
DOI: 10.1051/0004-6361:20053998

Astronomy & Astrophysics

Multifrequency VLA radio observations of the X-ray cavity cluster of galaxies RBS797: evidence of differently oriented jets

M. Gitti[1], L. Feretti[2], and S. Schindler[1]

[1] Institut für Astrophysik, Leopold-Franzens Universität Innsbruck, Technikerstraße 25, 6020 Innsbruck, Austria
e-mail: myriam.gitti@uibk.ac.at
[2] Istituto di Radioastronomia - INAF via Gobetti 101, 40129 Bologna, Italy

Received 5 August 2005 / Accepted 1 October 2005

ABSTRACT

We report on the peculiar activity of the radio source located at the center of the cooling flow cluster RBS797 ($z = 0.35$), the first distant cluster in which two pronounced X-ray cavities have been discovered. Our new multifrequency (1.4, 4.8, and 8.4 GHz) observations obtained with the Very Large Array clearly reveal the presence of radio emission on three different scales showing orientation in different directions, all of which indicates that RBS797 represents a very peculiar case. The lowest resolution images show large-scale radio emission characterized by amorphous morphology and a steep spectrum, extended on a scale of hundreds of kpc. On a scale of tens of kpc, there is evidence of 1.4 GHz radio emission elongated in the northeast-southwest direction exactly towards the holes detected in X-rays. The highest resolution image shows the details of the innermost 4.8 GHz radio jets on a kpc scale; they are remarkably oriented in a direction that is perpendicular to that of the extended structure detected at a lower resolution. We therefore find evidence of a strong interaction between the central radio source and the intra-cluster medium in RBS797. We suggest a scenario in which the 1.4 GHz emission filling the X-ray cavities consists of buoyant bubbles of radio emitting plasma that are created by twin jets in the past and whose expansion has displaced the thermal gas that was formerly in the X-ray holes, whereas the two jets visible at 4.8 GHz are related to the present nuclear activity that has restarted at a different position angle from the original outburst that created the outer radio lobes. The total radio luminosity is $\sim 10^{42}$ erg s^{-1}, corresponding to a factor of a few thousand times less than the estimated cooling luminosity.

Key words. galaxies: clusters: individual: RBS797 – radio continuum: galaxies – galaxies: active – galaxies: jets – X-rays: galaxies: clusters – galaxies: cooling flows

1. Introduction

An efficient cooling of the intra-cluster medium (ICM) is expected to occur in the clusters of galaxies with a sufficiently high gas density for the radiative cooling time due to X-ray emission to be shorter than the Hubble time (or the time since its last major merger). In the absence of any balancing heating mechanisms, the gas in the central regions of these clusters is expected to cool down and flow slowly inwards in order to maintain hydrostatic equilibrium (for a review of the standard *cooling flow* model, see Fabian 1994). Recent X-ray observations with *Chandra* and *XMM-Newton*, albeit confirming the existence of inwardly decreasing temperature gradients and short central cooling times, have altered this simple picture of steady cooling flows and show that little of the gas cools below ~1–2 keV (e.g. David et al. 2001; Johnston et al. 2002; Peterson et al. 2003, and references therein). The lack of observations of cooler gas represents an open question that is often referred to as the so called *"cooling flow problem"*.

Besides the hypothesis that the normal signatures of cooling below 1–2 keV are somehow suppressed[1], in order to avoid the expected rapid cooling to very low temperature, there must be some form of energy input into the ICM to balance the cooling. Currently the best candidates for supplying the energy are cluster-center radio sources that provide heating through processes associated with relativistic AGN outflows (e.g., Rosner & Tucker 1989; Tabor & Binney 1993; Churazov et al. 2001; Brüggen & Kaiser 2001; Kaiser & Binney 2002; Ruszkowski & Begelman 2002; Brighenti & Mathews 2003). Other proposed heating mechanisms include electron thermal conduction from the outer regions of clusters (Tucker & Rosner 1983; Voigt et al. 2002; Fabian et al. 2002b;

[1] Different possibilities have been investigated in this context, including: absorption (Peterson et al. 2001; Fabian et al. 2001), inhomogeneous metallicity (Fabian et al. 2001; Morris & Fabian 2003), the emerging of the missing X-ray luminosity in other bands, like ultraviolet, optical and infrared due to mixing with cooler gas/dust (Fabian et al. 2001, 2002a; Mathews & Brighenti 2003), and radio due to particle re–acceleration (Gitti et al. 2002, 2004).

Zakamska & Narayan 2003), continuous subcluster merging (Markevitch et al. 2001), contribution of the gravitational potential of the cluster core (Fabian 2003), feedback from intracluster supernovae (Domainko et al. 2004), etc.

As shown by Burns (1990), the vast majority of cooling flow clusters contain powerful radio sources associated with the central cD galaxies. These radio sources have a profound effect on the ICM, as the radio lobes displace the X-ray emitting gas, thereby creating X-ray deficient "holes" or "bubbles". High resolution X-ray images of cooling flows in galaxy clusters taken with *Chandra* indicate that indeed the central hot gas in these systems is not smoothly distributed but is cavitated on scales ranging from a few to a few tens of kpc, often approximately coincident with lobes of extended radio emission (e.g., Hydra A: McNamara et al. 2000; David et al. 2001; Allen et al. 2001; Perseus: Churazov et al. 2000; Böhringer et al. 1993; Fabian et al. 2000; A2052: Blanton et al. 2001, 2003; A2597: McNamara et al. 2001; RBS797: Schindler et al. 2001; De Filippis et al. 2002; A496: Dupke & White 2002; MKW 3s: Mazzotta et al. 2002; A2199: Johnstone et al. 2002; A4059: Heinz et al. 2002; Virgo: Young et al. 2002; Centaurus: Sanders & Fabian 2002; Cygnus A: Smith et al. 2002; A262: Blanton et al. 2004; A2597: Pollack et al. 2005; Clarke et al. 2005). Giant cavities, on scales of hundreds of kpc, have recently been found in the optically poor cluster MS0735.6+7241 (McNamara et al. 2005) and in Hercules A (Nulsen et al. 2005).

Comparisons of the total power emitted from the central radio source with the luminosity of cooling gas have shown that the energy emitted from a central radio source is sufficient to offset the cooling of the ICM in the centers of clusters, at least in some cases (e.g., Hydra A: David et al. 2001; A2052: Blanton et al. 2003). By performing a systematic study of radio-induced X-ray cavities, Bîrzan et al. (2004) show that the energy input from the central radio source is sufficient to balance cooling in roughly half of the 16 systems they study, at least for short time periods. It is interesting to note that the objects balancing the central cooling show a large spread in both radio luminosity and spectral index. The details of the transportation of the radio source energy to the ICM are still somehow obscure; however, the scenario of radio source heating remains a promising solution for the problem of the missing cool gas in the cooling flow model.

The X-ray luminous, distant galaxy cluster RBS797 (z = 0.35) was discovered in the ROSAT All-Sky Survey (Schwope et al. 2000). Observations with *Chandra* reveal two pronounced X-ray minima that are located opposite to each other with respect to the cluster center (Schindler et al. 2001). In the NRAO VLA Sky Survey (NVSS), an unresolved radio source of 20 mJy is present at the center of RBS797, and a spectrum of the central cluster galaxy shows emission lines; hence, the radio emission is likely to originate from an AGN. Preliminary results from low resolution VLA radio observations confirm the presence of a strong radio source positioned in the center of the cluster (De Filippis et al. 2002). As in the case of the X-ray holes observed in other clusters, the X-ray depressions detected in RBS797 suggest an interaction between the central radio galaxy and the ICM. This is a special case, though, since RBS797 has given us the chance to observe these features for the first time in a relatively distant cluster; and furthermore, the minima in this cluster are very symmetric and very deep compared to similar features found in other clusters.

Studying the interaction between the central radio galaxies of clusters and the ICM is of general interest, as such interaction can have numerous effects on the ICM. For example, the energy input from active galaxies into the ICM can be one of the reasons why poor clusters do not follow the general X-ray luminosity – temperature relation (Ponman et al. 1999). The additional non-gravitational heating required could be partly supplied by active galaxies. Furthermore, relativistic particles are injected into the ICM by active galaxies, and although they lose their energy to the ICM relatively fast, they might be re-accelerated later, probably in shock waves or turbulence generated by cluster mergers (e.g., Tribble 1993; Brunetti et al. 2001; Enßlin et al. 1998) or turbulence in the cooling flows (Gitti et al. 2002). These re-accelerated particles are very likely the source for the radio halos, relics, and mini-halos found in a number of galaxy clusters (for a more detailed discussion about diffuse radio emission observed in clusters see e.g., Feretti et al. 2004; and Kempner et al. 2004), and probably also for the non-thermal hard X-ray excess observed in some galaxy clusters (Fusco-Femiano 1999; 2001). Finally, the material transported from the galaxy into the ICM is probably metal-enriched, so that this process could contribute to the metal enrichment of the ICM. Typically, the metallicity of the ICM is about 0.3 solar; i.e. a lot of heavy elements must have been ejected by the cluster galaxies. Up to now it is not clear which of the suggested processes (galactic winds, ram-pressure stripping, galaxy-galaxy interaction, or ejection from active galaxies) is dominating at different redshifts (e.g., Schindler et al. 2005).

In this paper we present the VLA observations of the radio source in RBS797 and perform a detailed comparison of its structure with the structure of the ICM derived from earlier *Chandra* X-ray observations. In particular, we focus on the interaction between the radio source and the X-ray emitting ICM in order to get a comprehensive picture of the physical processes in clusters of galaxies. RSB797, whose central cluster galaxy is located at RA(J2000): $09^{\rm h}47^{\rm m}12\overset{\rm s}{.}5$, Dec(J2000): $76°23'14''0$, is at a redshift $z = 0.35$. With $H_0 = 70$ km s^{-1} Mpc^{-1}, and $\Omega_{\rm M} = 1 - \Omega_\Lambda = 0.3$, the luminosity distance is 1858 Mpc and 1 arcsec corresponds to 4.8 kpc. The radio spectral index α is defined as $S_\nu \propto \nu^\alpha$.

2. Observations and data reduction

Very Large Array[2] observations of the radio source RBS797 were made at three different frequencies (1.4 GHz, 4.8 GHz, 8.4 GHz) in different configurations (see Table 1 for details). In all observations the source 3C 286 was used as the primary flux density calibrator, while the sources 1044+809 and 0713+438 were used as secondary phase and polarization calibrators, respectively.

[2] The Very Large Array (VLA) is a facility of the National Radio Astronomy Observatory (NRAO). The NRAO is a facility of the National Science Foundation, operated under cooperative agreement by Associated Universities, Inc.

Table 1. VLA data archive.

Observation date	Frequency (MHz)	Bandwidth (MHz)	Array	Time (h)
Sep.-2001	8435/8485	50.0	D	5.0
Mar.-2002	1435/1515	50.0	A	4.5
Jul.-2002	1435/1515	50.0	B	4.8
Dec.-2004	4835/4885	50.0	A	7.0

Data reduction was done using the NRAO AIPS (Astronomical Image Processing System) package. Accurate editing of the uv data was applied to identify and remove bad data. At 1.4 GHz, only the channel centered at 1435 MHz was used because of strong interferences in the other channel. The 1.4 GHz data from the two different configurations were reduced separately, in order to analyze the possible existence of spurious features. Images at different resolutions were also obtained by adding the data together from the two configurations and by specifying appropriate values of the parameters UVTAPER and ROBUST in the AIPS task IMAGR. Images were produced by following the standard procedures: Calibration, Fourier-Transform, Clean and Restore. Self-calibration was applied to remove residual phase variations. Images in the Stokes parameters I, Q, and U were produced using the AIPS task IMAGR. The images of the polarized intensity, the fractional polarization, and the position angle of polarization were derived from the I, Q, and U images. The final images (Figs. 1, 2a–2c) show the contours of the total intensity.

3. Results

Figure 1 shows the radio map of RBS797 observed at 8.4 GHz with the VLA in D configuration, with a restoring beam of $6\farcs3 \times 3\farcs8$. The source shows an amorphous morphology elongated in the NE-SW direction with a total size of $\sim 25''$ (120 kpc). The source has a total flux density of $\simeq 3.02 \pm 0.03$ mJy, with a contribution of $\simeq 1.44 \pm 0.02$ mJy coming from the central $\sim 15''$ region. The source appears polarized at levels of $\simeq 10-20\%$ in a region extending $\sim 7'' \times 5''$ (34×24 kpc) out from the center.

Figure 2a shows the radio map of RBS797 observed at 1.4 GHz with the VLA in B configuration, with a restoring beam of $4\farcs9 \times 3\farcs8$. At this lower frequency and low resolution, the source shows its largest extent, with diffuse emission extended by approximately $45''$ (216 kpc) in the N-S direction and $\sim 30''$ (144 kpc) in the other direction. The morphology is quite regular, although slightly elongated to the north. The source has a total flux density of $\simeq 26.0 \pm 0.3$ mJy, with a contribution of $\simeq 11.5 \pm 0.1$ mJy coming from the central region. The source appears polarized at levels of $\simeq 10-20\%$ in a region extending $\sim 10'' \times 15''$ out from the center.

Figure 2b shows the radio map of RBS797 observed at 1.4 GHz with the VLA in A configuration with a restoring beam of $1\farcs5 \times 1\farcs1$. The higher resolution allows us to detect details of the central region. The source has a structure elongated in the NE-SW direction, as in the 8.4 GHz map presented in Fig. 1, although with a smaller total extent ($18'' \sim 86$ kpc).

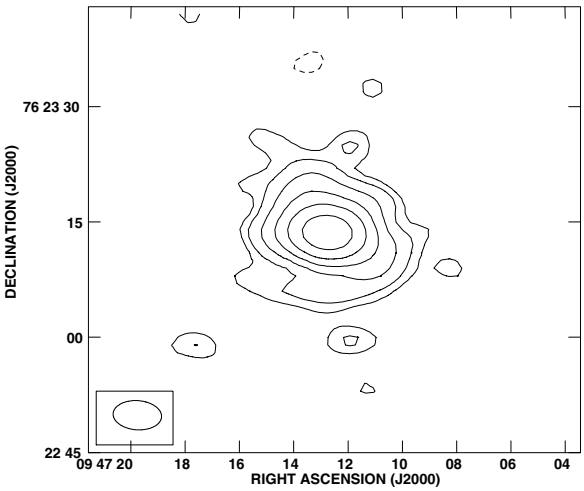

Fig. 1. 8.4 GHz VLA map of RBS797 at a resolution of $6\farcs3 \times 3\farcs8$ (the beam is shown in the lower lefthand corner). The contour levels are −0.03 (dashed), 0.03, 0.05, 0.10, 0.20, 0.40, 0.85, 1.70, 3.50 mJy/beam. The rms noise is 0.01 mJy/beam.

There is also a hint of possible faint jets emanating from the central component. The bright inner radio emission is resolved, showing an elongation along the N-S direction. The source has a total flux density of $\simeq 17.9 \pm 0.2$ mJy, with a contribution of $\simeq 12.1 \pm 0.1$ mJy coming from the central region (inner jets included, while the core alone has a flux density of $\simeq 10.8 \pm 0.1$ mJy). The central region appears polarized at levels of $\simeq 10-15\%$. Note that the structure shown here corresponds to the central $\sim 15''$(72 kpc) region in Fig. 2a, which has a total flux density of $\simeq 18.0 \pm 0.2$ mJy in agreement with these results at higher resolution.

The radio images presented in Figs. 2a and 2b have been obtained with the data from single configurations. We also obtained radio images at low ($\sim 5''$) and high ($\sim 1''$) resolution by adding together the data from the two configurations and by specifying appropriate values of the parameters in the AIPS task IMAGR (UVTAPER = 50, ROBUST = 5 and UVTAPER = 0, ROBUST = –5 for low and high resolution, respectively). The results are consistent with those obtained from single configurations. An image with the resolution of $\sim 3''$ was obtaiend from the combination of the data from the two configurations by setting UVTAPER = 60. This image (not shown here) is fully consistent with the other images presented in the paper.

Figure 2c shows the radio map of RBS797 observed at 4.8 GHz with the VLA in A configuration with a restoring beam of $0\farcs39 \times 0\farcs35$. The high resolution allows us to determine the position of the nucleus accurately, which is located at RA (J2000): $09^{h}47^{m}12\fs76$, Dec(J2000): $76°23'13\farcs74$.

The N-S elongation structure of the bright inner radio emission, detected in Fig. 2b, is fully unveiled here: the source clearly shows two jets pointing in the N-S direction and extending out from the core to a distance of approximately $2.8''$ (13.4 kpc). Two spots of enhanced brightness are visible at the outer edges of the jets. A feature extending to the west out to a distance of $\sim 1.9''$ (9 kpc) from the core is also visible ($\sim 5\sigma$ detection). The source has a total flux density of $\simeq 2.63 \pm 0.03$ mJy,

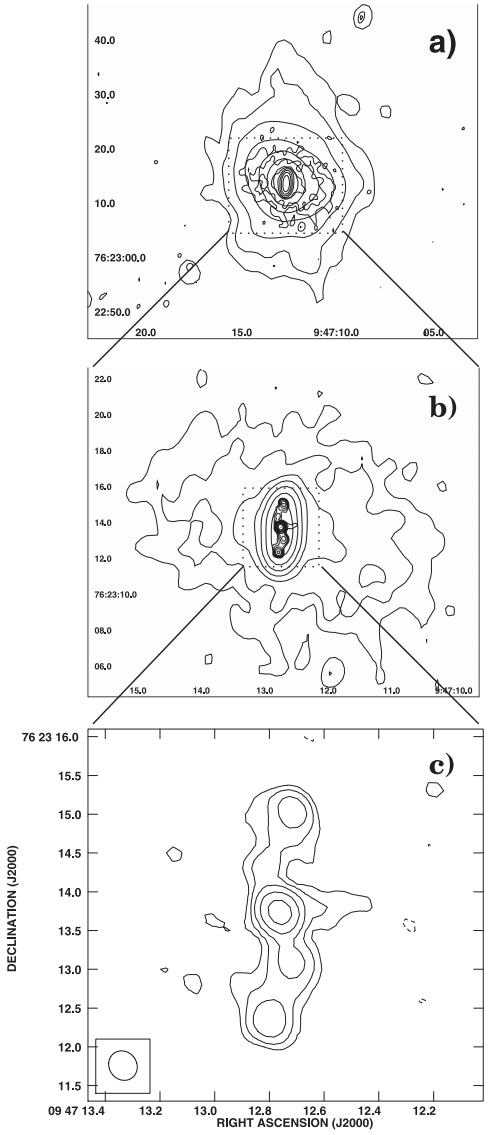

Fig. 2. Observations at different resolutions show orientations in different directions of the radio structures. The highest resolution image on kpc scale shows the details for the innermost 4.8 GHz radio jets, which clearly point to the N-S direction (panel **c)**). Remarkably, the inner jets are oriented in a direction almost perpendicular to that of the extended structure detected at lower resolution, which is elongated in the NE-SW direction (panel **b**)). The lowest resolution images show large-scale radio emission with amorphous morphology, slightly extended in the N-S direction (see panel **a)**). See text (Sect. 4) for more details. **a)** Black contours: 1.4 GHz VLA map of RBS797 at a resolution of $4\farcs9 \times 3\farcs8$. The contour levels are −0.08 (dashed), 0.08, 0.15, 0.30, 0.60, 1.20, 2.50 mJy/beam. The rms noise is 0.03 mJy/beam. Overlayed in grey are the 1.4 GHz contour plot at ∼1″ resolution (the beam and rms noise are the same as in **b)**. **b)** Black contours: 1.4 GHz VLA map of RBS797 at a resolution of $1\farcs5 \times 1\farcs1$. The contour levels are −0.05 (dashed), 0.05, 0.10, 0.20, 0.40, 0.80, 1.50, 3.00 mJy/beam. The rms noise is 0.02 mJy/beam. Overlayed in grey are the 4.8 GHz contour plot at ∼0.″4 resolution (the beam and rms noise are the same as in **c)**. **c)** 4.8 GHz VLA map of RBS797 at a resolution of $0\farcs39 \times 0\farcs35$ (the beam is shown in the lower-left corner). The contour levels are −0.04 (dashed), 0.04, 0.08, 0.16, 0.32, 0.64, 1.28, 2.50 mJy/beam. The rms noise is 0.01 mJy/beam.

with a contribution of ≃0.83 ± 0.02 mJy coming from the nuclear region. The central region and the two brighter spots appear strongly polarized at levels of ≃10−35%.

Very remarkable is that the two jets visible in Fig. 2c are oriented in a direction perpendicular to that of the extended structures detected at lower resolution (Figs. 1 and 2b). In order to show the relation of the diffuse structure to the finer scale structure detected at higher resolution, we display in Fig. 2a the overlay of the 1.4 GHz map at ∼4″ resolution onto the 1.4 GHz map at ∼1″ resolution, and then in Fig. 2b the overlay of the same 1.4 GHz map at arcsec resolution onto the 4.8 GHz map at subarcsec resolution.

The radio results are summarized in Table 2, where we also report the monochromatic radio power at each frequency calculated as

$$P_\nu = 4\pi D_{\rm L}^2 S_\nu (1+z)^{-(\alpha+1)} \quad (1)$$

where $D_{\rm L}$ is the luminosity distance, S_ν the flux density in Janskys[3] at the frequency ν, and $(1+z)^{-(\alpha+1)}$ the *K-correction* term (Petrosian & Dickey 1973), which in our case is negligible ($\alpha \sim -1$).

3.1. Spectral index

The dependence of the source's appearance on frequency and resolution reflects both the diffuse nature of the extended emission and the steep, but position-dependent, spectrum of the radio emission. By comparing the peak flux densities at 8.4 GHz in array D, 1.4 GHz in array B, and the total flux density at 4.8 GHz in array A, we estimated that the central region has a spectral index of $\alpha_{4.8}^{8.4} = -0.98 \pm 0.03$, $\alpha_{1.4}^{4.8} = -1.09 \pm 0.01$, and $\alpha_{1.4}^{8.4} = -1.06 \pm 0.01$. We note that these spectral values, which refer to the emission visible in Fig. 2a, are steeper than those commonly expected in nuclear-jet structures.

In Fig. 3 we show a greyscale of the spectral index map between 8.4 and 1.4 GHz at ∼4.5″ resolution[4] superposed on the 8.4 GHz total intensity contours. Besides confirming the steep spectrum ($\alpha \sim -1$) of the central region, this figure shows the general trend of the spectrum of the diffuse emission to steepen toward the outer region ($\alpha \simeq -1$ to $\simeq -1.5$). We estimated that the very low brightness emission extended to the north at 1.4 GHz in array B (Fig. 2a) has a steep spectral index $\alpha \lesssim -1.5$, by assuming an upper limit of 3σ for the 8.4 GHz flux.

4. Discussion

4.1. X-rays

The cluster RBS797 was observed in 2000 with the *Chandra* Advanced CCD Imaging Spectrometer (ACIS) I detector (Schindler et al. 2001). The smoothed X-ray image (0.5–7 keV) produced from these data is shown in Fig. 4. At large radii,

[3] 1 Jy = 10^{-26} W Hz^{-1} m^{-2}.

[4] The imaging procedure at each frequency (8.4 GHz in array A and 1.4 GHz in array A+B combined) was performed using data with matched uv coverage.

Table 2. Radio results for RBS797.

Freq. (GHz)	Array	Beam ($''$)	Size ($''^2$)	rms (mJy/beam)	Peak (mJy/beam)	Total flux (mJy)	Radio power (10^{24} W Hz^{-1})	Flux central emission (mJy)
8.4	D	6.31×3.79	28×25	0.009	1.53	3.02 ± 0.03	1.24 ± 0.01	1.44 ± 0.02
1.4	B	4.94×3.81	44×30	0.027	9.94	26.04 ± 0.26	10.7 ± 0.11	11.49 ± 0.12
1.4	A	1.52×1.14	18×11	0.017	4.83	17.90 ± 0.18	7.38 ± 0.07	10.75 ± 0.11
4.8	A	0.39×0.35	5.5×1.5	0.013	0.98	2.63 ± 0.03	1.08 ± 0.01	0.83 ± 0.02

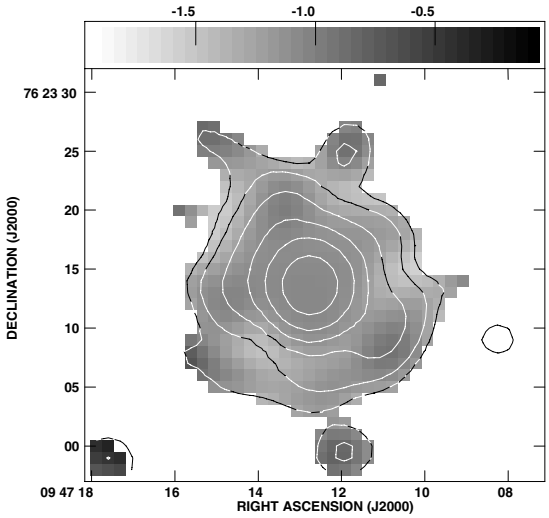

Fig. 3. Spectral index distribution between $\nu = 8.4$ GHz and $\nu = 1.4$ GHz at a resolution of $4''.5 \times 4''.5$. The lighter the grey, the steeper the spectral index. We excluded the region in which the error is >0.2. Superposed are the contours of the 8.4 GHz total intensity (with the same levels as in Fig. 1).

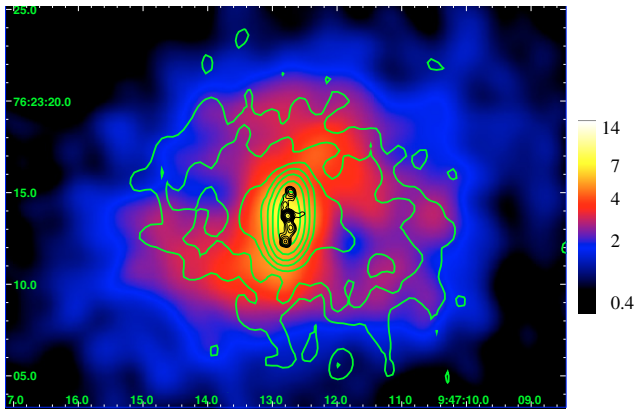

Fig. 4. 1.4 GHz (green) and 4.8 GHz (black) radio contours overlaid onto the *Chandra* X-ray image (0.5–7 keV) of the central region of RBS797. The X-ray surface brightness image, in units of cts/s/arcmin^2, is smoothed with a Gaussian of $\sigma = 0.75$ arcsec.

RBS797 shows a very regular morphology, looking fairly relaxed with a slight elliptical shape. The inner part of the cluster shows the high surface brightness characteristic of a cooling flow, even though there might be contamination due to the emission of a central AGN (Schindler et al. 2001). At small radii, the X-ray emission shows a peculiar structure instead, with two strong depressions in the NE-SW direction at distances of about 3–5 arcsec from the cluster center. The minima are opposite to each other with respect to the cluster center. In perpendicular directions, a bar of enhanced X-ray emission is visible: the surface brightness at radii of 4 arcsec is a factor of 3–4 lower in the minima compared to the perpendicular directions, which corresponds to about 20 counts in each minimum and 70 counts in the same area in perpendicular directions (Schindler et al. 2001). The X-ray depressions, which have a size of about 15–25 kpc[5], are surrounded by a bright ring of emission. The brightest parts of the ring and bar appear to form two shells to the NE and SW.

A recent re-analysis of these data was performed by Bîrzan et al. (2004), who find a cooling radius $r_{\rm cool} \sim 190$ kpc. By making a deprojected spectral analysis, they estimated a spectroscopic cooling luminosity $L_{\rm spec} \sim 1.2 \times 10^{45}$ erg s^{-1} and a total luminosity inside the cooling radius $L_{\rm X} \sim 4.5 \times 10^{45}$ erg s^{-1}. A visual inspection of the X-ray image led them to infer a size of $\sim 10 \times 10$ kpc and $\sim 14 \times 9$ kpc for the two cavities, located at a projected distance from the radio core of ~20 kpc and ~24 kpc, respectively. The ratio of the pV work done on the surrounding medium by the cavity (calculated from measurements of the cavity volume and gas pressure) to the age of the cavity gives the instantaneous mechanical luminosity. By assuming for the age the time required for the cavity to rise buoyantly at its terminal velocity, Bîrzan et al. (2004) estimate a mechanical luminosity for the cavity pair observed in RBS797 of $L_{\rm mech} \sim 2.8 \times 10^{44}$ erg s^{-1}.

4.2. Radio

The multifrequency VLA observations of RBS797 presented in Sect. 3 clearly reveal the presence of radio emission on three different scales. The lowest resolution images show diffuse radio emission extended on a scale of hundreds of kpc (see Figs. 1 and 2a). The size of the extended radio emission, which is characterized by amorphous morphology and a steep spectrum that steepens with distance from the center, is roughly comparable to that of the cooling region (Bîrzan et al. 2004). These characteristics point to a possible classification of the diffuse radio source as a mini-halo. In addition to radio halos and relics, radio mini-halos represent another class of diffuse radio sources associated with the ICM. They have low surface brightness, steep spectrum, and they are extended on a scale up to ~500 kpc, surrounding a dominant radio galaxy at the cluster center. They are only observed in clusters with a cooling flow.

Besides the large-scale emission, radio emission extended on a scale of tens of kpc is detected at arcsec resolution

[5] Quantities were scaled accordingly to the value of H_0 adopted.

(Fig. 2b). In particular, there is clear evidence of the presence of a bright inner radio emission that is surrounded by a more extended, fainter emission elongated in the NE-SW direction. Observations at even higher (subarcsec) resolution allow us to clearly distinguish the innermost radio jets on the kpc scale (Fig. 2c) that point to the N-S direction.

4.3. X-ray – radio interaction

The new radio images presented here for RBS797 led us to classify the cavities observed in X-rays as radio-filled cavities, contrary to their classification as ghosts in the sample by Bîrzan et al. (2004). The classification as radio-filled cavities appears evident in Fig. 4, where the 1.4 GHz radio contours are overlaid onto the *Chandra* X-ray image of the inner region of RBS797.

It is very interesting to note that the radio structure is elongated exactly towards the holes detected in the X-ray emission; in particular, most of the extended radio emission is projected within the X-ray holes to the NE-SW. Almost all of the radio emission is contained within the bright X-ray shells. Besides the 1.4 GHz radio contours at arcsec resolution, in Fig. 4 we also show the 4.8 GHz radio contours at subarcsec resolution overlaid onto the *Chandra* X-ray image. This radio-X overlay is indicative of a strong interaction between the ICM and the radio source embedded in the central cluster galaxy. In particular, it suggests that the expansion of the 1.4 GHz radio source has displaced the thermal gas that was formerly in the X-ray holes and compressed this gas into the bright shells. On the other hand, it is very remarkable that the two jets visible at 4.8 GHz are oriented in a direction perpendicular to the cavities, thus indicating that either the jet axes have been deflected from their original directions into the outer lobes or the renewed activity has begun at a different position angle from the original outburst that created the outer radio lobes. If confirmed, the small 4.8 GHz structure visible at high resolution extending to the west of the nucleus perpendicular to the main jet axis (see Fig. 2c) could be related to the one observed on a larger scale at 1.4 GHz (see Fig. 2b).

The structure extending in the NE-SW direction, visible at 1.4 GHz in Fig. 4 may originate by the deflection of the inner jets visible at 4.8 GHz (Fig. 4) oriented in the N-S direction. A deflected jet scenario has been investigated in the case of the radio source PKS 2322−123 located at the center of the cooling flow cluster A2597 (Pollack et al. 2005).

An alternative theory to that of a deflected jet is a precessing radio jet, as described by Gower et al. (1982). In this scenario, the current stage of RBS797 could lead to the creation of future "ghost cavities", which are thought to be buoyant lobes from a past outburst of the radio galaxy and which have displaced the thermal gas as they rose through the cluster atmosphere. Observational evidence suggests that radio galaxies undergo episodic outbursts that last $\sim 10^7$ yr and also have repetition intervals of $\sim 10^8$ yr (e.g., McNamara et al. 2001). Over the cluster lifetime, the activity of the central radio galaxy would produce many generations of radio lobes. This is consistent with the observation both of the random location of older, more distant bubbles and the irregular X-ray images within the central few kpc of some galaxy clusters (e.g. Perseus: Churazov et al. 2000; Böhringer et al. 1993; Fabian et al. 2000), which are apparently inconsistent with nonthermal jets having fixed orientations defined by the spin axis of massive black holes (Brighenti & Mathews 2002).

Precessing inner jets could be explained in the context of binary black hole models. The presence of a binary black hole in a galactic nucleus may indeed become manifest through precession of a jet propagation along the rotation axis of the primary, more massive black hole during a period of activity (Begelman et al. 1980). Hence, relativistic material ejected in different episodes of outbursts may be expelled in different directions from the central engine similar to the radio directions in the observations here. The picture of RBS797 harboring a supermassive binary black hole might be further strengthened by the small feature extending to the west in Fig. 2c, which could itself be interpreted as ejecta originating from the secondary black hole.

As discussed above, the different radio jet orientation observed in RBS797 could be explained either by deflection or precession. For both these cases, one important question is how violent and energetic the expansion of the radio source after the outburst is. Heinz et al. (1998) and Rizza et al. (2000) suggested that the radio source would create cavities in the ICM by highly supersonic expansion into the gas and that such a violent expansion would drive strong shocks into the ICM. Due to the compression in the shocks, the shell of X-ray gas surrounding the radio-filled cavity would have a higher temperature, pressure, and specific entropy than would the gas just outside the shell. This model seems to be ruled out in the case of the 1.4 GHz radio source in RBS797, as Schindler et al. (2001) find a slightly lower temperature in the bright shells than for the rest of the cluster. Since the gas in the shells is denser than the ICM outside the shells, the specific entropy ($S \propto \mathrm{T}n^{-2/3}$) is actually much lower than outside the shells, suggesting that the shells are probably not shocked regions. Thus, the expansion of the radio source is probably subsonic or mildly transonic, as found in other clusters, such as Hydra A (McNamara et al. 2000; David et al. 2001), Perseus (Fabian et al. 2000), and A2052 (Blanton et al. 2001). However, due to the short exposure time of the *Chandra* observation, it is not possible to derive a temperature map, which would be essential for distinguishing different models. Furthermore, one might expect the X-ray gas to have equal or greater pressure than the non-thermal gas, which would be consistent with the hypothesis of a confined radio jet. Unfortunately with the X-ray data currently available, it is not possible to perform an accurate study of the pressure balance between the X-ray emitting gas and the innermost radio source in RBS797.

One possible qualitative interpretation we can infer from the present data is that the 1.4 GHz emission extending to the NE-SW from the center consists of bubbles of radio-emitting plasma created by twin jets in the past, which are moving away from the center due to buoyancy, while the two jets visible at 4.8 GHz are related to current nuclear activity. The qualitative picture is that a past radio activity may have injected radio-emitting plasma that then propagates through the cooling flow region in the form of buoyant subsonic plumes. During the

initial phase, the jets inflate the cocoon with relativistic plasma, and the expansion is supersonic, while at a later stage the expansion slows down and becomes subsonic. On the other hand, buoyancy limits the growth of the cavities inflated by the jets, and when the rising velocity due to buoyancy exceeds the expansion velocity, the bubble detaches from the jet and begins rising (Churazov et al. 2000). As shown by several authors who have studied the hydrodynamic evolution of rising bubbles (e.g. Gull & Northover 1973; Churazov et al. 2000; Brüggen & Kaiser 2001), the moving away from the center is accompanied by adiabatic expansion and further mixing of the energetic radio source material with the ambient ICM. This latter process occurs via Kelvin-Helmholtz (K-H) instabilities on the surface of the bubbles and, more importantly, via Rayleigh-Taylor (R-T) instabilities on the "top" surface of the bubble that will actually disrupt and fragment it. Hydrodynamic simulations show a dramatic breakup and fine-scale mixing of the bubble material with the ICM in about 10^7–10^8 years (e.g. Brüggen & Kaiser 2002). This is comparable to (or bigger than) the lifetime of the electrons that produce synchrotron radiation[6]. Electrons emitting at frequencies ∼1 GHz in magnetic fields on the order of ∼1–3 μG, typical for the ICM, have a radiative lifetime of $\sim 7 \times 10^7$ yr.

The disruption of the bubbles produced in past radio outbursts would then have left a population of relic relativistic electrons mixed with the thermal plasma in the cooling flow region. These relic electrons could diffuse in the thermal plasma up to ∼100 kpc scale in a few Gyr (e.g., Brunetti 2003) filling the whole region observed in Fig. 2a and thus forming the population of relic electrons required by the re-acceleration model for the origin of radio mini-halos[7] (Gitti et al. 2002, 2004). In particular, analogous to the case of the Perseus cluster, it might be difficult to find a direct connection between the inner radio lobes and the large-scale extended emission in terms of simple buoyancy or particle diffusion, since the expansion and buoyancy of blobs would produce adiabatic losses and a decrease in the magnetic field causing too strong a steepening of the spectrum, which would in turn prevent detection of large-scale radio emission. Thus, if the relativistic electrons are of primary origin, efficient re-acceleration mechanisms in the cooling flow region are necessary to explain the presence of the large-scale radio emission. A detailed application to RBS797 of the model for the origin of radio mini-halos consisting of MHD turbulent re-acceleration of intra-cluster cosmic ray electrons (Gitti et al. 2002, 2004) will be presented in a forthcoming paper.

[6] The radiative lifetime of an ensemble of relativistic electrons losing energy by synchrotron emission and inverse Compton (IC) scattering off the CMB photons, defined such as $\tau = -E/\dot{E}$, is given by (e.g., Ginzburg & Syrovatskii 1965; Rybicki & Lightman 1979):

$$\tau_{\rm sin+IC} \simeq \frac{2.5 \times 10^{13}}{\left[(B/\mu{\rm G})^2 + (B_{\rm CMB}/\mu{\rm G})^2\right] \gamma} \quad {\rm yr}$$

where B is the magnetic field intensity, γ the Lorentz factor, and $B_{\rm CMB} = 3.18(1+z)^2$ μG the magnetic field equivalent to the CMB in terms of electron radiative losses.

[7] Alternatively, Pfrommer & Enßlin (2004) suggest that radio mini-halos may be of hadronic origin from cosmic rays.

4.4. Can radio source heating quench the cooling?

By assuming a spectral index $\alpha = -1$, we calculated the total radio luminosity of the full source visible in Fig. 2a over the frequency range of 10 MHz–10 GHz to be $L_{\rm radio} \sim 10^{42}$ erg s^{-1}. In order to investigate whether the radio source deposits enough energy into the ICM to quench cooling, this has to be compared with the cooling luminosity. As derived by Bîrzan et al. (2004) in the case of RBS797, the cooling luminosity is $L_{\rm X} - L_{\rm spec} \sim 3.3 \times 10^{45}$ erg s^{-1}, therefore the radio source is too weak by a factor of a few thousand to balance cooling in this system.

On the other hand, it is well known that radio sources are inefficient radiators and that the mechanical (kinetic) luminosity $L_{\rm mech}$ of radio sources can be much higher than their synchrotron luminosity. One way to estimate $L_{\rm mech}$ is through measurements of the X-ray cavity size and surrounding gas pressure, as done by Bîrzan et al. (2004) for a sample of cavity clusters. In particular, these authors derive a value of $L_{\rm mech} \sim 2.8 \times 10^{44}$ erg s^{-1} for the cavity pair observed in RBS797. We estimated the radio luminosity corresponding to the radio structure visible at 1.4 GHz in array A (Fig. 4) to be $\sim 7.1 \times 10^{41}$ erg s^{-1}. The mechanical luminosity $L_{\rm mech}$ is thus ∼400 times the observed radio luminosity of the radio source filling the X-ray cavities. Even considering the total mechanical luminosity of the central radio source, as estimated from the cavity properties, it seems that cooling cannot be balanced by bubble heating in the galaxy cluster RBS797.

5. Conclusions

We have presented multifrequency (1.4, 4.8, and 8.4 GHz) VLA observations of the radio source located at the center of the cooling flow cluster RBS797 ($z = 0.35$), which is the first distant cluster in which two pronounced X-ray depressions have been discovered by previous *Chandra* observations (Schindler et al. 2001). We detected radio emission on three different scales showing orientation in different directions, thus indicating that RBS797 represents a very peculiar case.

The highest resolution image on kpc scale shows the details of the innermost 4.8 GHz radio jets, which point clearly to the N-S direction. Remarkably, the inner jets are oriented in a direction almost perpendicular to that of the extended structure detected at lower resolution, which is elongated in the NE-SW direction exactly towards the holes detected in X-rays. The lowest resolution images show large-scale radio emission with amorphous morphology, slightly extended in the N-S direction. We therefore find evidence of a strong interaction between the central radio source and the intra-cluster medium in RBS797.

Further observations in X-rays and radio are needed to either rule out or confirm the models that we have suggested for the interaction between the radio source and the X-ray gas. In particular, more detailed investigations of the innermost structure of this source will add an important piece of information for investigating the energetics involved in the formation of cavities in the X-ray gas and in the process of interaction between the radio sources and the ambient gas.

Acknowledgements. We thank W. Domainko for suggesting the possibility of RBS797 harboring a binary black hole, and G. Hasinger for

useful discussions. We also thank the anonymous referee for useful comments. M.G. would like to thank F. Brighenti for many stimulating discussions and insightful comments. This work was supported by the Austrian Science Foundation FWF under grant P15868 and by the Tiroler Wissenschaftsfonds.

References

Allen, S. W., Taylor, G. B., Nulsen, P. E. J., et al. 2001, MNRAS, 324, 842
Begelman, M. C., Blandford, R. D., & Rees, M. J. 1980, Nature, 287, 307
Bîrzan, L., Rafferty, D. A., McNamara, B. R., Wise, M. W., & Nulsen, P. E. J. 2004, ApJ, 607, 800
Blanton, E. L., Sarazin, C. L., McNamara, B. R., & Wise, M. W. 2001, ApJ, 558, L15
Blanton, E. L., Sarazin, C. L., & McNamara, B. R. 2003, ApJ, 585, 227
Blanton, E. L., Sarazin, C. L., McNamara, B. R., & Clarke, T. E. 2004, ApJ, 612, 817
Böhringer, H., Voges, W., Fabian, A. C., Edge, A. C., & Neumann, D. N. 1993, MNRAS, 264, L25
Brighenti, F., & Mathews, W. G. 2002, ApJ, 574, L11
Brighenti, F., & Mathews, W. G. 2003, ApJ, 587, 580
Brüggen, M., & Kaiser, C. R. 2001, MNRAS, 325, 676
Brüggen, M., & Kaiser, C. R. 2002, Nature, 418, 301
Brunetti, G. 2003, Proc. of the Conf. on Matter and Energy in Clusters of Galaxies held on April 23–27, 2002 in Chung-Li, Taiwan; ed. S. Bowyer, & C.-Y. Hwang, ASP Conf. Ser., 301, 349
Brunetti, G., Setti, G., Feretti, L., & Giovannini, G. 2001, MNRAS, 320, 365
Burns, J. O. 1990, AJ, 99, 14
Churazov, E., Forman, W., Jones, C., & Böhringer, H. 2000, A&A, 356, 788
Churazov, E., Brüggen, M., Kaiser, C. R., Böhringer, H., & Forman, W. 2001, ApJ, 554, 261
Clarke, T. E., Sarazin, C. L., Blanton, E. L., Neumann, D. M., & Kassim, N. E. 2005, ApJ, 625, 748
David, L. P., Nulsen, P. E. J., McNamara, B. R., et al. 2001, ApJ, 557, 546
De Filippis, E., Schindler, S., & Castillo-Morales, A. 2002, Proc. of the Symp. New Visions of the X-ray Universe in the XMM-Newton and Chandra era, Noordwijk [arXiv:astro-ph/0201349]
Domainko, W., Gitti, M., Schindler, S., & Kapferer, W. 2004, A&A, 425, L21
Dupke, R., & White, R. E. III 2002, in High Energy Universe at Sharp Focus: Chandra Science, ed. E. M. Schlegel, & S. Vrtilek (San Francisco: ASP), ASP Conf. Ser., 262, 51
Enßlin, T. A., Biermann, P. L., Klein, U., & Kohle, S. 1998, A&A, 332, 395
Fabian, A. C. 1994, ARA&A, 32, 277
Fabian, A. C. 2003, MNRAS, 344, L27
Fabian, A. C., Sanders, J. S., Ettori, S., et al. 2000, MNRAS, 318, L65
Fabian, A. C., Mushotsky, R. F., Nulsen, P. E. J., & Peterson, J. R. 2001, MNRAS, 321, L20
Fabian, A. C., Allen, S. W., Crawford, C. S., et al. 2002a, MNRAS, 332, L50
Fabian, A. C., Voigt, L. M., & Morris, R. G. 2002b, MNRAS, 335, L71
Feretti, L., Burigana, C., & Enßlin, T. A. 2004, New Astron. Rev., 48, 1137
Fusco-Femiano, R., Dal Fiume, D., Feretti, L., et al. 1999, ApJ, 513, L21
Fusco-Femiano, R., Dal Fiume, D., Orlandini, M., et al. 2001, ApJ, 552, L97
Ginzburg, V. L., & Syrovatskii, S. I. 1965, ARA&A, 3, 297
Gitti, M., Brunetti, G., & Setti, G. 2002, A&A, 386, 456
Gitti, M., Brunetti, G., Feretti, L., & Setti, G. 2004, A&A, 417, 1
Gower, A. C., Gregory, P. C., Hutchings, J. B., & Unruh, W. G. 1982, ApJ, 262, 478
Gull, S. F., & Northover, K. J. E. 1973, Nature, 244, 80
Heinz, S., Reynolds, C. S., & Begelman, M. C. 1998, ApJ, 501, 126
Heinz, S., Choi, Y.-Y., Reynolds, C. S., & Begelman, M. C. 2002, ApJ, 569, L79
Johnstone, R. M., Allen, S. W., Fabian, A. C., & Sanders, J. S. 2002, MNRAS, 336, 299
Kaiser, C., & Binney, J. 2002, MNRAS, 338, 837
Kempner, J. C., Blanton, E. L., Clarke, T. E., et al. 2004, in The Riddle of Cooling Flows in Galaxies and Clusters of Galaxies, ed. T. H. Reiprich, J. C. Kempner, & N. Soker, http://www.astro.virginia.edu/coolflow/
Markevitch, M., Vikhlinin, A., & Mazzotta, P. 2001, ApJ, 562, L153
Mathews, W. G., & Brighenti, F. 2003, ApJ, 590, 5
Mazzotta, P., Kaastra, J. S., Paerels, F. B., et al. 2002, ApJ, 567, L37
McNamara, B. R., Wise, M., Nulsen, P. E. J., et al. 2000, ApJ, 534, L135
McNamara, B. R., Wise, M. W., Nulsen, P. E. J., et al. 2001, ApJ, 562, L149
McNamara, B. R., Nulsen, P. E. J., Wise, M. W., et al. 2005, Nature, 433, 45
Morris, R. G., & Fabian, A. C. 2003, MNRAS, 338, 824
Nulsen, P. E. J., Hambrick, D. C., McNamara, B. R., et al. 2005, ApJ, 625, L9
Peterson, J. R., Paerels, F. B. S., Kaastra, J. S., et al. 2001, A&A, 365, L104
Peterson, J. R., Kahn, S. M., Paerels, F. B. S., et al. 2003, ApJ, 590, 207
Petrosian, V., & Dickey, J. 1973, ApJ, 186, 403
Pfrommer, C., & Enßlin, T. 2004, A&A, 413, 17
Pollack, L. K., Taylor, G. B., & Allen, S. W. 2005, MNRAS, 359, 1229
Ponman, T. J., Cannon, D. B., & Navarro, J. F. 1999, Nature, 397, 135
Rybicki, G. B., & Lightman, A. P. 1979, Radiative Processes in Astrophysics (Wiley-Interscience Pub.)
Rizza, E., Loken, C., Bliton, M., Roettiger, K., & Burns, J. O. 2000, AJ, 119, 21
Rosner, R., & Tucker, W. 1989, ApJ, 338, 761
Ruszkowski, M., & Begelman, M. C. 2002, ApJ, 586, 384
Sanders, J. S., & Fabian, A. C. 2002, MNRAS, 331, 273
Schindler, S., Castillo-Morales, A., De Filippis, E., Schwope, A., & Wambsganss, J. 2001, A&A, 376, L27
Schindler, S., Kapferer, W., Domainko, W., et al. 2005, A&A, 435, L25
Schwope A., Hasinger, G., Lehmann, I., et al. 2000, AN, 321, 1
Smith, D. A., Wilson, A. S., Arnaud, K. A., Terashima, Y., & Young, A. G. 2002, ApJ, 565, 195
Tabor, G., & Binney, J. 1993, MNRAS, 263, 323
Tribble, P. C. 1993, MNRAS, 263, 31
Tucker, W. H., & Rosner, R. 1983, ApJ, 267, 547
Voigt, L. M., Schmidt, R. W., Fabian, A. C., Allen, S. W., & Johnstone, R. M. 2002, MNRAS, 355, 7
Young, A. J., Wilson, A. S., & Mundell, C. G. 2002, ApJ, 579, 560
Zakamska, N., & Narayan, R. 2003, ApJ, 582, 162